Article

Current Biology

Claustral Neurons Projecting to Frontal Cortex Mediate Contextual Association of Reward

Graphical Abstract

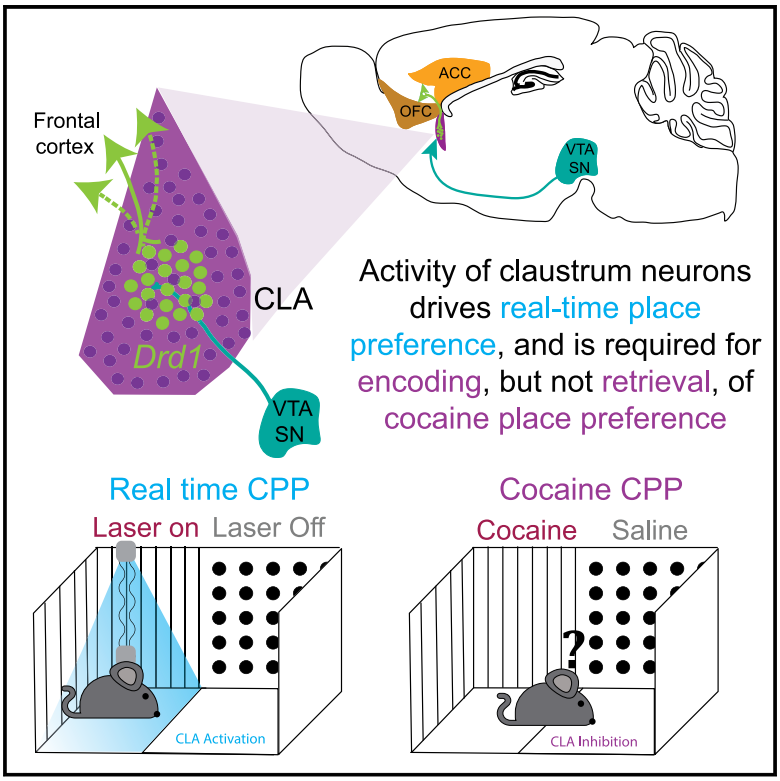

Authors

Anna Terem, Ben Jerry Gonzales, Noa Peretz-Rivlin, ..., Diptendu Mukherjee, Maya Groysman, Ami Citri

Correspondence

ami.citri@mail.huji.ac.il

In Brief

Terem et al. uncover the role of the claustrum in context reinforcement. They identify claustral dopamine D1-receptor-expressing neurons as a subpopulation of frontal-projecting claustral neurons important for *de novo* context reinforcement and the acquisition of cocaine preference.

Highlights

- The claustrum receives dopamine inputs and expresses dopamine receptors
- Claustral D1R^{+} cell activity is required for acquisition of cocaine preference
- D1R^{+} neurons are a subset of frontal-projecting claustral neurons
- Stimulation of claustrum D1R^{+}/frontal-projecting cells drives context conditioning

Terem et al., 2020, Current Biology *30*, 1–11
September 21, 2020
https://doi.org/10.1016/j.cub.2020.06.064

CellPress

Please cite this article in press as: Terem et al., Claustral Neurons Projecting to Frontal Cortex Mediate Contextual Association of Reward, Current Biology (2020), https://doi.org/10.1016/j.cub.2020.06.064

Current Biology

CellPress
OPEN ACCESS

Article

Claustral Neurons Projecting to Frontal Cortex Mediate Contextual Association of Reward

Anna Terem,[1,2] Ben Jerry Gonzales,[1,2] Noa Peretz-Rivlin,[1] Reut Ashwal-Fluss,[1,2] Noa Bleistein,[1,2] Maria del Mar Reus-Garcia,[3] Diptendu Mukherjee,[1,2] Maya Groysman,[1] and Ami Citri[1,2,4,5,*]

[1]The Edmond and Lily Safra Center for Brain Sciences, The Hebrew University of Jerusalem, Edmond J. Safra Campus, Givat Ram, Jerusalem 9190401, Israel

[2]Institute of Life Sciences, The Hebrew University of Jerusalem, Edmond J. Safra Campus, Givat Ram, Jerusalem 9190401, Israel

[3]Division of Neurosciences, Pablo de Olavide University, Seville 41013, Spain

[4]Program in Child and Brain Development, Canadian Institute for Advanced Research, MaRS Centre, West Tower, 661 University Avenue, Suite 505, Toronto, ON M5G 1M1, Canada

[5]Lead Contact

*Correspondence: ami.citri@mail.huji.ac.il

https://doi.org/10.1016/j.cub.2020.06.064

SUMMARY

The claustrum is a small nucleus, exhibiting vast reciprocal connectivity with cortical, subcortical, and midbrain regions. Recent studies, including ours, implicate the claustrum in salience detection and attention. In the current study, we develop an iterative functional investigation of the claustrum, guided by quantitative spatial transcriptional analysis. Using this approach, we identify a circuit involving dopamine-receptor expressing claustral neurons projecting to frontal cortex necessary for context association of reward. We describe the recruitment of claustral neurons by cocaine and their role in drug sensitization. In order to characterize the circuit within which these neurons are embedded, we apply chemo- and opto-genetic manipulation of increasingly specified claustral subpopulations. This strategy resolves the role of a defined network of claustrum neurons expressing dopamine D1 receptors and projecting to frontal cortex in the acquisition of cocaine conditioned-place preference and real-time optogenetic conditioned-place preference. In sum, our results suggest a role for a claustrum-to-frontal cortex circuit in the attribution of incentive salience, allocating attention to reward-related contextual cues.

INTRODUCTION

The claustrum is a small subcortical nucleus, exhibiting vast reciprocal connectivity with large regions of cortex, as well as with many subcortical and midbrain structures [1–8]. The function of the claustrum has been the subject of much speculation [1–4, 9,10–12], with recent observations identifying roles for the claustrum in salience detection and attention [8, 13–20]. The claustrum has also been recognized as a major hub of neuromodulatory action in the brain, uniquely enriched in expression of receptors for many classes of neuromodulators, and receiving inputs from multiple neuromodulatory structures [1–4, 21, 22]. Dopaminergic innervation of the claustrum has been indicated from studies across mammalian species [21–25], including reports of projections to the claustrum from midbrain dopamine centers [13, 21, 22, 26, 27] as well as tyrosine hydroxylase (TH) staining in the claustrum [21–25, 28]. Claustral expression of dopamine receptors has been reported, as have functional responses to dopamine within the claustrum [25, 28–35]. This dopaminergic innervation of the claustrum has been hypothesized to function in supporting reinforcement and the acquisition of reward [9, 26]. The association of dopamine reward and attention evoke the concept of incentive salience, which is defined as a form of motivational salience, by which attention is allocated in a dopamine-dependent manner to cues associated with reward [36, 37]. The reported roles of the claustrum in salience detection and attention, together with its dopaminergic modulation, position the claustrum as a candidate structure for the attribution of incentive salience.

The most prominent long-range connectivity of the claustrum is with frontal cortical structures. Inputs to the claustrum from frontal cortex have been implicated in attention [5, 38, 39], whereas claustral input to frontal structures is reported to provide robust feedforward inhibition [40, 41]. The action of claustrum on frontal circuits has been suggested to provide a large-scale form of lateral inhibition, whereby claustral neurons suppress designated cortical regions. This lateral inhibition has been proposed to reduce the representation of irrelevant sensory information, permitting context-specific cortical circuits to encode stimuli according to behavioral demands [4, 13, 40].

In this study, we find that the activity of the claustrum is necessary for the development of behavioral sensitization to cocaine. We report that the claustrum receives dopamine inputs and expresses dopamine receptors and that claustral neurons expressing D1 dopamine receptors are preferentially recruited by cocaine. Furthermore, activity of $D1R^{+}$ claustral neurons is required for the development of cocaine conditioned-place preference (CPP), and their optogenetic activation can drive the development of place preference. Finally, we find that $D1R^{+}$ claustral neurons project to frontal cortex, and the activity of

Please cite this article in press as: Terem et al., Claustral Neurons Projecting to Frontal Cortex Mediate Contextual Association of Reward, Current Biology (2020), https://doi.org/10.1016/j.cub.2020.06.064

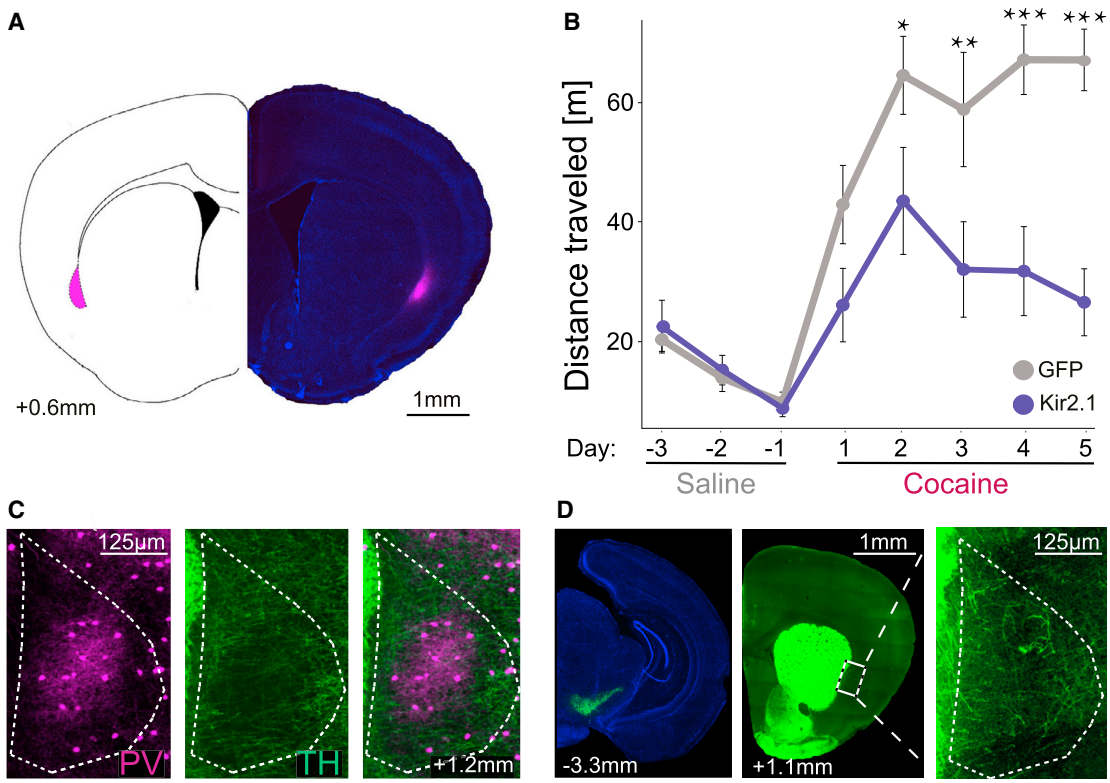

Figure 1. The claustrum receives dopaminergic input and inhibition of claustral neurons attenuates behavioral sensitization to cocaine

(A) Example section demonstrating the domain of viral transduction after stereotactic targeting of AAVdj-CAG-DIO-GPE2 (Cre-dependent Kir2.1) to the claustrum region of Egr2-Cre mice.

(B) Constitutive inhibition of CL_{Egr2+} neurons attenuates the development of behavioral sensitization to cocaine. Egr2-Cre mice were injected bilaterally with viruses conditionally expressing Kir2.1 (n = 9) versus GFP (n = 6) as control. Mice were habituated to an open field arena and saline injection (i.p.) for 3 days, followed by 5 days of cocaine exposure (20 mg/kg, i.p.) (linear regression model comparing GFP to Kir2.1, *p < 0.05, **p < 0.01, ***p < 0.001).

(C) Tyrosine hydroxylase (TH) staining in the claustrum of PV-Cre:Ai9 mice. The claustrum core is defined by its rich PV^+neuropil in sections from the Ai9xPV-Cre mouse line (magenta). Staining for TH reveals catecholaminergic innervation of the claustrum (green), preferentially innervating the claustrum shell surrounding the PV-rich core (overlay; right). The source of the saturated signal on the left side of the images is the dense TH^+ innervation of the striatum.

(D) The claustrum receives dopaminergic input from midbrain dopamine neurons. Stereotactic targeting of AAV-DIO-GFP to the midbrain of DAT-Cre mice (left panel) labels dopamine axons in the claustrum (middle; expanded view in right graphic; see also Figure S1).

frontal-projecting claustral neurons is essential for the development of cocaine conditioned place preference, whereas their activation drives place preference. Our results suggest a role for D1R-expressing frontal-projecting claustral neurons in the attribution of incentive salience.

RESULTS

Inhibition of claustrum neurons attenuates behavioral sensitization to cocaine

We chose to investigate the role of the claustrum in the development of cocaine-driven behaviors because of the high efficiency of these experimental models of drug sensitization and reward, and their obvious societal implications. We first studied the role of the claustrum in cocaine sensitization, a paradigm that measures progressive increase in drug-induced behaviors, by inhibiting the activity of claustral *Egr2*$^+$ neurons (CL_{Egr2+}) prior to cocaine exposure. Constitutive inhibition of the claustrum was achieved by conditional expression of the inward rectifying K^+ channel Kir2.1 in CL_{Egr2+}, as previously characterized [13] (Figure 1). In contrast to control mice (expressing GFP in CL_{Egr2+}), which developed the expected locomotor sensitization after repeated daily exposure to cocaine (20 mg/kg, i.p.), inhibition of CL_{Egr2+} neurons clearly limited the development of cocaine sensitization (Figure 1B). Applying a linear regression model that considered the interaction of experimental group with experimental day (as explained in the STAR Methods and Data S1) demonstrated that sensitization was impacted in claustrum-inhibited mice ($F_{7,84} = 5.5$, $p < 0.0001$, ANOVA). This effect can be observed from the first day of cocaine exposure (albeit not reaching statistical significance in comparison to control mice, $p = 0.06$), and the distinction between control and experimental mice becomes more prominent after additional exposures to cocaine. This result implicates the claustrum in mediating locomotor sensitization to repeated cocaine exposures.

The claustrum receives dopaminergic inputs

The identification of a role of the claustrum in cocaine sensitization motivated us to characterize the dopaminergic system of the claustrum and address the role of this structure in mouse models

Please cite this article in press as: Terem et al., Claustral Neurons Projecting to Frontal Cortex Mediate Contextual Association of Reward, Current Biology (2020), https://doi.org/10.1016/j.cub.2020.06.064

CellPress
OPEN ACCESS

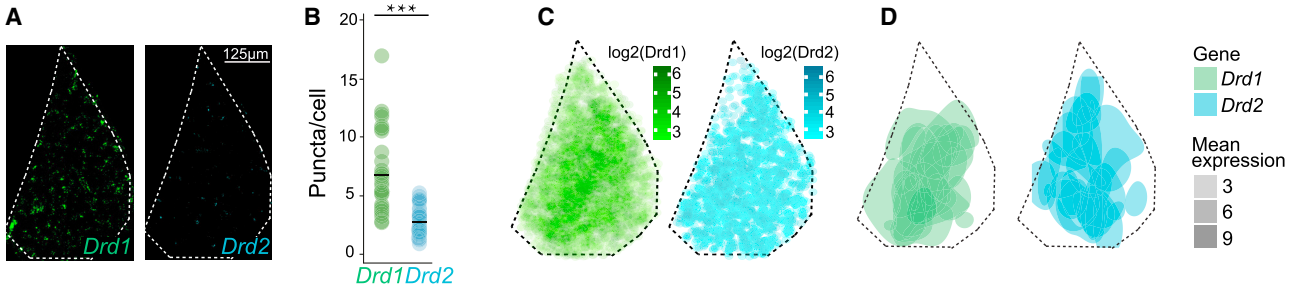

Figure 2. Dopamine receptor expression in the claustrum

(A) Representative images of single-molecule fluorescence *in situ* hybridization (smFISH) staining in the claustrum, demonstrating robust expression of *Drd1*, contrasting with sporadic *Drd2* expression.

(B) Average cellular expression of *Drd1* and *Drd2* in claustral cells. Student's t test ***p < 0.001 (puncta per cell; n = 33 sections).

(C) Spatial distribution of *Drd1* and *Drd2* in the claustrum. Digitized representation of the distribution of $Drd1^+$ and $Drd2^+$ neurons in the claustrum (*Drd1*/*Drd2* threshold ≥6 puncta per cell; overlay of 33 digitized sections).

(D) *Drd1* expression is enriched toward the center of the claustrum. Two-dimensional kernel density estimation was used to demarcate regions of maximal density of high expressing cells, demonstrating hotspots of receptor expression in the claustrum. see also Figure S2.

of cocaine reward. We performed TH immunostaining in order to study the catecholaminergic innervation of the claustrum in mice. As a reference for the identification of the claustrum, we contrasted TH staining with the dense neuropil of parvalbumin (PV; labeling the claustrum core), visualized in PV-Cre:Ai9 mice (expressing tdTomato in PV^+ interneurons) [38, 42, 43]. TH-expressing neuropil was observed throughout the claustrum, and there was reduced intensity in the PV-rich claustrum core (Figure 1C). In order to verify that the TH staining of the claustrum corresponds to dopaminergic axons, we stereotactically targeted an adeno-associated virus (*AAV*) conditionally expressing GFP (AAV_{dj}-DIO-GFP) to the midbrain of DAT-IRES-Cre knockin mice. These mice conditionally express Cre recombinase under the regulation of the dopamine transporter gene *Slc6a3*, enabling genetic access to dopamine-producing neurons. This strategy demonstrated dopamine inputs to the mouse claustrum, in a pattern similar to the one obtained by TH staining (Figure 1D). These results are further corroborated by data from the Allen Brain Mouse Connectivity Atlas (Figure S1). Thus, multiple sources of evidence suggest that the claustrum receives dopaminergic input from the midbrain, consistent with our previous report of inputs to the claustrum from midbrain dopamine centers [13, 26, 44].

Claustral dopamine receptor expression

We next addressed the claustral expression of dopamine receptors, utilizing multi-colored single-molecule *in situ* hybridization (smFISH). Our results demonstrate robust cellular expression of the *Drd1* dopamine receptor in claustral neurons, as well as sparse modest expression of *Drd2* (Figure 2A). Claustral neurons express on average 7.2 ± 0.6 puncta per cell of *Drd1*, and 3.1 ± 0.2 puncta per cell of *Drd2* (Figure 2B, $p < 0.0001$, t test). The threshold to define $Drd1^+$ or $Drd2^+$ cells was set at ≥6 puncta, defining 45% ± 3% of claustral cells as $Drd1^+$ and 15% ± 1% as $Drd2^+$ (Figure S2A) ($p < 0.0001$, t test). Although claustral expression of *Drd1* and *Drd2* is uncorrelated at the single-cell level (Figure S2B) ($r^2 = 0.07$, $p < 0.0001$), the majority (60% ± 5%) of $Drd2^+$ neurons also express *Drd1*, whereas a minority (17% ± 4%) of $Drd1^+$ neurons co-express *Drd2*. Studying the spatial distribution of claustral dopamine receptor expression in the claustrum, we observe *Drd1* throughout the claustrum, enriched toward the middle of the claustrum, whereas the relatively modest expression of *Drd2* appears to be more evenly distributed throughout the claustrum (Figures 2C and 2D). Qualitatively similar claustral dopamine receptor patterns were reported in a recent study performed in rats [25].

Cocaine drives induction of immediate-early genes in claustral $Drd1^+$ cells

We next studied the recruitment of claustral neurons by cocaine, by assaying immediate-early gene (IEG) expression in the claustrum, and its correlation with dopamine receptor expression, at different stages of the development of behavioral sensitization to cocaine. We addressed the expression of *Fos*, the canonical IEG, as well as *Egr2*, which is expressed in claustral neurons [13] and modulated by cocaine [45, 46]. Acute, repeated, and challenge exposure to cocaine were studied, eliciting the anticipated sensitization of locomotion behavior (Figure 3A). Although the claustral expression of *Drd1* and *Drd2* is not affected by cocaine exposure (Figures S2C and S2D) ($F_{2,30} = 0.69$, $p = 0.52$ and $F_{2,30} = 0.035$, $p = 0.9$, respectively, one-way ANOVA), induction of *Egr2* is observed in the claustrum after acute exposure to cocaine (Figure 3B) ($p = 0.007$, t test). Further, the expression of both *Egr2* and *Fos* is robustly induced after repeated ($p < 0.0001$ for both, t test), as well as challenge cocaine exposures (*Egr2* $p = 0.003$, *Fos* $p = 0.009$, t test). Notably, repeated exposure to cocaine drives hyper-reactivation of the transcriptional induction of both *Egr2* and *Fos* (Figure S3A) (sum expression: *Egr2* acute: 2.3 ± 0.4-fold induction, repeated: 4- ± 0.3-fold induction; $F_{2,23} = 8.5$, $p = 0.002$, one-way ANOVA followed by Tukey's test; *Fos* acute: 1.3 ± 0.2-fold induction, repeated: 2.9 ± 0.2-fold induction; $F_{2,15} = 16.1$, $p = 0.0002$, one-way ANOVA followed by Tukey's test). The spatial pattern of *Egr2* and *Fos* induction mirrors the spatial distribution of *Drd1* in the claustrum, given that these genes exhibited a broad distribution and an apparent preference for the center of the claustrum (Figures 3C–3E). The per-cell expression of *Egr2* and *Fos* is correlated in basal conditions, as well as after exposure to cocaine (Figures S3C–S3G), reminiscent of our recent observations regarding IEG induction patterns in the striatum after acute

Please cite this article in press as: Terem et al., Claustral Neurons Projecting to Frontal Cortex Mediate Contextual Association of Reward, Current Biology (2020), https://doi.org/10.1016/j.cub.2020.06.064

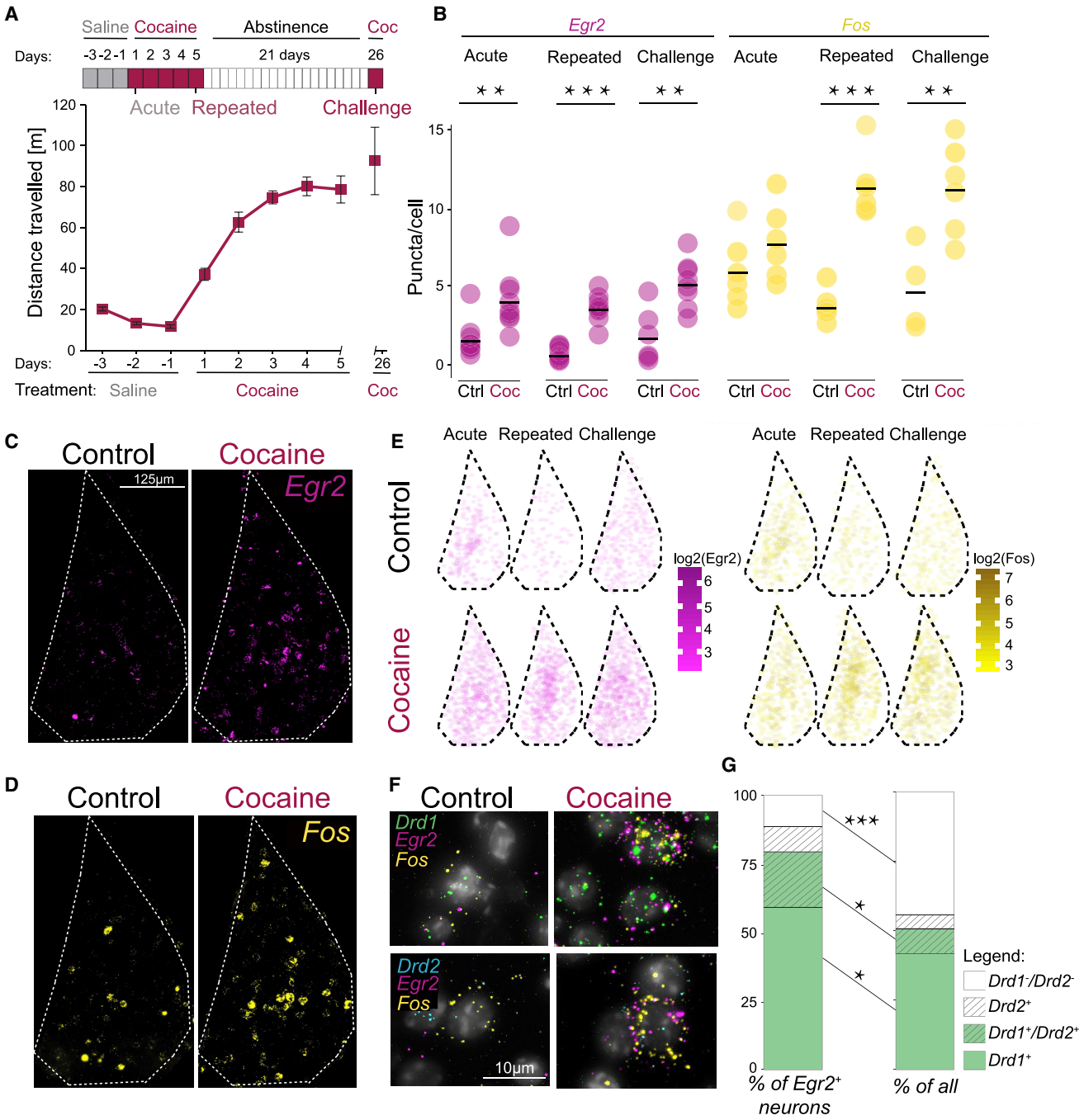

Figure 3. Cocaine drives induction of immediate-early genes in claustral *Drd1*$^+$ cells

(A) Scheme depicting protocol for acute, repeated, and challenge exposure of mice to cocaine (20 mg/kg, i.p.), as well as the locomotion analyzed for these mice (acute: n = 15, repeated: n = 12, challenge: n = 3 mice).

(B) Induction of *Egr2* and *Fos* after acute, repeated, and challenge exposures to cocaine. *Egr2*: acute (0 h; n = 9, 1 h; n = 9), repeated (0 h; n = 9, 1 h; n = 9), challenge (0 h; n = 6, 1 h; n = 8, *Fos*: acute (0 h; n = 6, 1 h; n = 6), repeated (0 h; n = 6, 1 h; n = 6), challenge (0 h; n = 4, 1 h; n = 6); n number refers to number of sections analyzed. Student's t test **p < 0.01, ***p < 0.001.

(C and D) Representative images demonstrating claustral expression of *Egr2* (C) and *Fos* (D) in control versus after acute exposure to cocaine.

(E) Digitized spatial distribution of *Egr2*$^+$ and *Fos*$^+$ cells in the claustrum in control versus after acute, repeated, and challenge exposure to cocaine. Cells are color coded according to the level of cellular expression. *Egr2* threshold >4 puncta per cell, overlay of 50 digitized sections; *Fos* threshold >7 puncta per cell, overlay of 34 digitized sections.

(F) High-magnification 40× images depicting co-expression of *Drd1, Egr2*, and *Fos* versus *Drd2*, *Egr2*, and *Fos* in claustral cells under control conditions as well as after acute exposure to cocaine.

(legend continued on next page)

Please cite this article in press as: Terem et al., Claustral Neurons Projecting to Frontal Cortex Mediate Contextual Association of Reward, Current Biology (2020), https://doi.org/10.1016/j.cub.2020.06.064

cocaine exposure [46]. Addressing the identity of neurons within which *Egr2* is expressed (Figures 3F, 3G, and S3C–S3G), we observed enrichment of *Egr2* expression within claustral dopamine receptor-expressing neurons ($p < 0.0001$, chi-square test). In fact, 87% ± 3% of *Egr2*-expressing neurons are positive for dopamine receptor expression, in comparison to 56% ± 5% of total claustral cells ($p < 0.0001$, t test). Of *Egr2*$^+$ cells, 61% ± 5% are *Drd1*$^+$; 17% ± 4% *Drd1*$^+$*Drd2*$^+$ and 9% ± 2% *Drd2*$^+$, whereas 13% ± 3% express neither *Drd1* nor *Drd2*. In comparison to total claustral cells, of which 42% ± 5% express *Drd1*$^+$; 9% ± 2% *Drd1*$^+$*Drd2*$^+$; 5% ± 1% *Drd2*$^+$ and 44% ± 5% express neither *Drd1* nor *Drd2* (*Drd1*$^+$ $p = 0.02$; *Drd1*$^+$*Drd2*$^+$ $p = 0.05$; *Drd1*$^-$*Drd2*$^-$ $p < 0.0001$, t test) (Figure 3G). *Egr2* expression is most prominently observed correlated with *Drd1* expression, but a small subset of *Drd2*-expressing neurons (70% ± 6% of which co-express *Drd1*) also exhibit a correlation between dopamine receptor expression and *Egr2* expression (Figure S3D). Furthermore, 62% ± 3% of *Fos*$^+$ cells co-express *Drd1*, in contrast to the background of 39% ± 3% of total cells expressing *Drd1*, whereas 15% ± 2% of *Fos*$^+$ cells co-express *Drd2*, in comparison to 16% ± 2% of total cells expressing *Drd2* (*Drd1*$^+$ $p < 0.0001$; *Drd2*$^+$ $p = 0.69$; t test).

Thus, cocaine exposure preferentially recruits *Drd1*$^+$ claustral neurons, driving robust induction of IEG expression within them. Notably, this IEG induction is sensitized by repeated exposure to cocaine.

Activity of claustral D1R$^+$ neurons is essential for the acquisition of cocaine CPP and drives the development of real-time place preference

The enrichment of cocaine-induced IEG expression within *Drd1*$^+$ neurons suggests that these neurons might be involved in the development of cocaine preference. In order to functionally interrogate the role of claustral *Drd1*$^+$ neurons in the development of CPP for cocaine (Figure 4A), we bilaterally injected Cre-dependent viral constructs to the claustrum region of D1-Cre mice (transgenic mice expressing the Cre recombinase under the regulation of the *Drd1* promoter) (Figure 4B). Using this approach, we obtained transduction efficiency of 20%–53% of claustral neurons across a variety of viral constructs, with minimal leakage to the striatum (for delineation of expression domains, see Figures 4B and S4). We initiated analysis of the role of claustral *Drd1*$^+$ neurons in supporting cocaine CPP by constitutively inhibiting their firing through conditional expression of Kir2.1 (Figures 4C and S4A). Although the control group of mice (conditionally expressing GFP) developed preference for the cocaine-associated context, mice expressing Kir2.1 in claustral D1R$^+$ neurons failed to develop CPP (control $p < 0.0001$; Kir2.1 $p = 0.26$; paired t test). In order to clarify whether the activity of claustral neurons is required for the acquisition of cocaine CPP or its expression, we utilized conditional chemogenetic inhibition (with the DREADD hM4Di, as previously characterized [13]). To address the role of claustral *Drd1*$^+$ neurons in acquisition of cocaine preference, mice were exposed to the hM4Di ligand CNO (10 mg/kg, i.p.) prior to cocaine conditioning (Figures 4D and S4B). Although control groups of mice (conditionally expressing GFP and treated with CNO, or expressing hM4Di and treated with saline) developed CPP (GFP/CNO $p = 0.01$; hM4Di/saline $p = 0.003$, paired t test), selective inhibition of claustral *Drd1*$^+$ neurons during acquisition of cocaine preference attenuated the development of CPP ($p = 0.37$, paired t test). A different cohort of mice was used to test the role of claustral *Drd1*$^+$ neurons in the expression of cocaine CPP. In this experiment, after an initial test to verify the development of prominent CPP, mice were subject to an additional conditioning round and exposed to CNO prior to a final preference test. Both control and experimental groups of mice developed CPP (WT: $F_{2,12} = 34.9$, $p < 0.0001$; hM4Di: $F_{2,8} = 24$, $p = 0.0004$, two-way ANOVA using the between-subjects factor of the mouse and within-subjects factor of the experiment day), and claustral inhibition had no effect on the expression of CPP (Figures 4E and S4C). Thus, claustral *Drd1*$^+$ neurons are selectively recruited to support the acquisition of cocaine preference, but their activity is dispensable for its expression.

If the claustrum plays a role in the attribution of incentive salience, we expect mice to develop preference for a context coupled to activation of the claustrum. To address this question, we studied the capacity of claustral neurons to drive the development of real-time CPP for optogenetic stimulation (rtCPP [47]). In this experiment, mice were placed in a 3-compartment chamber and closed-loop optogenetic stimulation of claustral neurons was triggered whenever the mouse entered a defined compartment (Figure 4F). Bilateral expression of ChR2 in claustral *Drd1*$^+$ neurons drove the development of optogenetic real-time preference for the compartment coupled to optogenetic stimulation (Figure 4G) ($F_{3,21} = 3.5$, $p = 0.003$, two-way ANOVA using the between-subjects factor of the mouse and within-subjects factor of the experiment day; for location of virus transduction and fiber placement see Figure S4D). Preference for the laser-coupled side developed during the first session of stimulation, and continued to develop on a consecutive day of stimulation. Furthermore, a preference test performed on the following day (in the absence of laser stimulation) demonstrated retention of conditioned preference for the chamber coupled to optogenetic stimulation.

Thus, claustral *Drd1*$^+$ neuronal activity is required for the acquisition of cocaine conditioned-place preference, whereas activation of these neurons is sufficient to support real-time place preference. When considered in light of the cumulative literature connecting the claustrum with salience detection and selective attention [13–19], these results support a role for the claustrum in attribution of incentive salience to cocaine-associated contextual cues.

Frontal-projecting claustral neurons are enriched for *Drd1*$^+$ expression, required for acquisition of cocaine CPP and support the development of real-time place preference

The bilateral communication of the claustrum with frontal cortex is the most prominent feature of claustral long-range

(G) Distribution of *Drd1*$^+$ or *Drd2*$^+$ cells as a fraction of *Egr2*$^+$ cells versus total claustral cells. Of *Egr2*$^+$ cells, 61% ± 5% are *Drd1*$^+$; 17% ± 4% *Drd1*$^+$*Drd2*$^+$ and 9% ± 2% *Drd2*$^+$, whereas 13% ± 3% express neither *Drd1* nor *Drd2*. In comparison, of all claustral cells, 42% ± 5% express *Drd1*$^+$; 9% ± 2% *Drd1*$^+$*Drd2*$^+$; 5% ± 1% *Drd2*$^+$ and 44% ± 5% express neither *Drd1* nor *Drd2*. *$p < 0.05$, ***$p < 0.0001$; t test; see also Figure S3.

Please cite this article in press as: Terem et al., Claustral Neurons Projecting to Frontal Cortex Mediate Contextual Association of Reward, Current Biology (2020), https://doi.org/10.1016/j.cub.2020.06.064

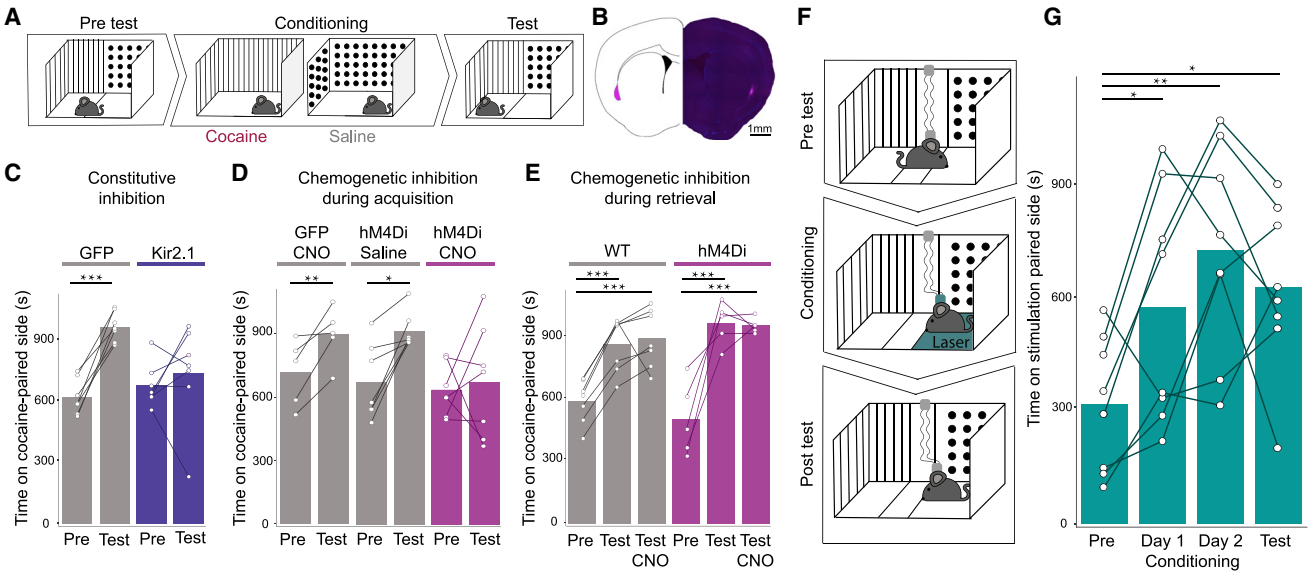

Figure 4. Activity of claustral D1R$^+$ neurons is essential for the acquisition of cocaine CPP and drives the development of real-time place preference

(A) Scheme of experimental paradigm for testing conditioned-place preference for cocaine. The arena is comprised of two compartments, distinct in the pattern printed on the walls, as well as the texture of the flooring. The initial preference of mice for either context is tested, after which the mice are repeatedly conditioned, daily, for 3 days, to cocaine (10 mg/kg, i.p.) in one context versus saline (i.p.) in the other context. On the final day, the preference of the mice for either compartment is tested.

(B) Representative example of selective conditional virus-mediated expression in the claustrum of a D1-Cre mouse.

(C) Constitutive inhibition of *Drd1*$^+$ claustral neurons prevents the development of cocaine conditioned-place preference (CPP). Time spent in the cocaine-paired context is plotted, with the bar demonstrating the group mean, and individual mice depicted as connected circles (GFP control n = 7; Kir2.1 n = 7, paired t test).

(D) Selective chemogenetic inhibition of claustral *Drd1*$^+$ neurons during acquisition blocks the development of cocaine CPP. Exposure to CNO (10 mg/kg, i.p.) 30 min prior to cocaine conditioning inhibited the development of CPP in mice expressing the hM4Di DREADD in claustral *Drd1*$^+$ neurons. A control group of mice expressing GFP in claustral neurons developed CPP, as did a second control group, expressing hM4Di and exposed to saline prior to cocaine conditioning (GFP/CNO n = 5; hM4Di/saline n = 7; hM4Di/CNO n = 7, paired t test; see Data S1).

(E) Selective chemogenetic inhibition of *Drd1*$^+$ claustral neurons during expression of CPP does not impact the expression of CPP. Both control and hM4Di-expressing groups of mice were initially tested and, after an additional day of conditioning, re-tested after exposure to CNO, which did not impact the development of CPP (control n = 7; hM4Di n = 5, WT n = 7; hM4Di n = 5, linear regression model including the mouse and day effects; see Data S1).

(F) Scheme of layout of real-time optogenetic place conditioning experiment. Following recovery from surgery for virus transduction and fiber optic cannula implantation, the initial preference of mice was tested in a 3-chamber arena. On the following days, closed-loop optogenetic stimulation was delivered every time the mouse crossed into the stimulation-paired context (parameters: 20 Hz (duty cycle 5 ms on/45 ms off) for 1 s on/3 s off, 5 mA). On the test day, the mice were queried for their side preference.

(G) Optogenetic stimulation of claustral *Drd1*-expressing neurons drives the development of real-time CPP (n = 8, linear regression model including the mouse and day effects; see Data S1). *p < 0.05, **p < 0.01, ***p < 0.001. See also Figures S4 and S5D.

connectivity [8, 13, 40, 43, 48–50]. Frontal inputs to the claustrum have been associated with salience detection and selective attention [8, 13, 15–19]. Moreover, claustral inputs to frontal cortex have been implicated in feedforward inhibition, putatively increasing contrast of cortical activity, favoring the representation of stimuli prioritized for attention [40]. The majority of claustral neurons are excitatory projection neurons, positive for expression of *Slc17a7*/vGlut1 [13]. Accordingly, claustral D1R$^+$ neurons constitute a subpopulation of claustral projection neurons (Figures 5A and 5B) (89% of all claustral cells and 93% of *Drd1*$^+$ cells express vGlut1). Utilizing retrograde-trafficking AAV viruses, we selectively accessed claustral neurons projecting to frontal cortical regions (orbitofrontal cortex [OFC] and anterior cingulate cortex [ACC]) (Figures 5C and 5D). Studying the dopamine receptor expression profile of frontal projection neurons, we find that dopamine-receptor expressing claustral neurons constitute a subset of frontal-projecting claustral neurons. Whereas frontal-projecting neurons capture 58% ± 3% of total claustral cells, 92% ± 1% of *Drd1*$^+$ and 94% ± 4% of *Drd2*$^+$ claustral neurons project to frontal cortex (Figures 5E, 5F, and S5A). This result demonstrates that the claustral projection to frontal cortex is selectively enriched with dopamine sensitivity ($p < 0.0001$ for both *Drd1*$^+$ and *Drd2*$^+$, chi-square test), potentially functioning to promote cocaine-driven behavior. In order to address this possibility, we targeted frontal-projecting claustral neurons by stereotactic injection of a retro-transporting retroAAV-iCre bilaterally to the ACC and OFC, intersected with bilateral injection of AAV-DIO-hM4Di virus to the claustrum. We tested the role of frontal-projecting neurons in the acquisition of cocaine CPP, by conditionally inhibiting their activity during cocaine place conditioning (Figures 5G and S5B). Whereas control groups developed prominent CPP (GFP/CNO $p = 0.04$; hM4Di/saline $p = 0.0007$, paired t test), conditional inhibition of frontal-projecting claustral neurons significantly attenuated the

Please cite this article in press as: Terem et al., Claustral Neurons Projecting to Frontal Cortex Mediate Contextual Association of Reward, Current Biology (2020), https://doi.org/10.1016/j.cub.2020.06.064

CellPress
OPEN ACCESS

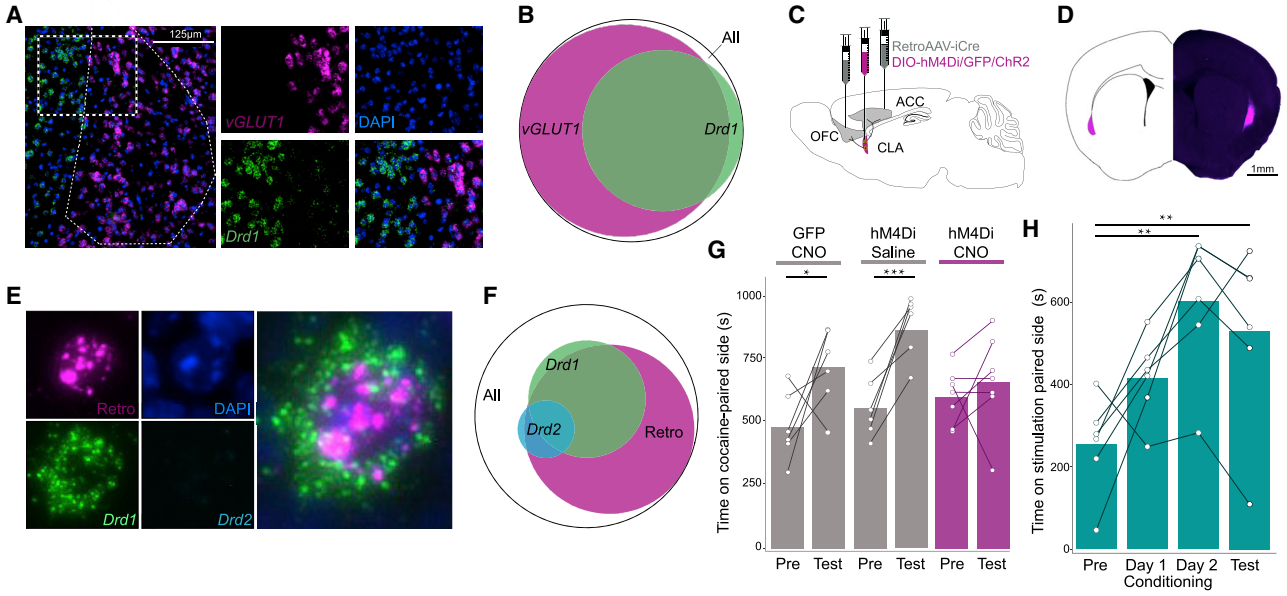

Figure 5. Frontal-projecting claustral neurons are enriched for *Drd1*$^+$ expression, required for acquisition of cocaine CPP and drive the development of real-time place preference

(A) Representative low-magnification 10× images of smFISH staining, demonstrating co-expression of *Drd1* and *vGlut1* in claustral neurons.

(B) Venn diagram quantifying the percentage of *vGlut1*$^+$ and *Drd1*$^+$ of total claustral neurons. 89% of claustral cells are *vGlut1*$^+$, whereas 56% are *Drd1*$^+$, 93% of *Drd1*$^+$ are *vGlut1*$^+$, whereas 59% of *vGlut1*$^+$ neurons are *Drd1*$^+$ (of all = 48.6% *Drd1*$^+$*vGlut1*$^+$, 41% *Drd1*$^-$*vGlut1*$^+$, 3.5% *Drd1*$^+$*vGlut1*$^-$, 6.9% *Drd1*$^-$*vGlut1*$^-$).

(C) Schematic representation of strategy of retrograde labeling of claustral neurons projecting to frontal cortical structures. The retrogradely transporting virus retro-AAV-iCre was injected bilaterally into the anterior cingulate cortex (ACC) and orbitofrontal cortex (OFC) of mice and intersected with transduction of the claustral region with viruses conditionally expressing hM4Di-mCherry, GFP, or ChR2.

(D) Representative example of expression in the claustral region of retroAAV-iCre-targeted mice intersected with transduction of the claustral region with a virus conditionally expressing hM4Di-mCherry.

(E) Representative high-magnification 40× images of smFISH staining, demonstrating co-expression of *Drd1* with retrogradely labeled claustral neurons.

(F) Venn diagram quantifying the percentage of *Drd1*$^+$ versus retrogradely labeled claustral neurons, of total claustral neurons. 58% of claustral cells were retrogradely labeled, within which were found 92% ± 1% of *Drd1*$^+$ cells and 94% ± 4% of *Drd2*$^+$ cells (of all = 39.5% Retro$^-$*Drd1*$^-$*Drd2*$^-$, 30.2% Retro$^+$*Drd1*$^-$*Drd2*$^-$, 21.4% Retro$^+$*Drd1*$^+$*Drd2*$^-$, 4.1% Retro$^+$*Drd1*$^+$*Drd2*$^+$, 2.1% Retro$^-$*Drd1*$^+$*Drd2*$^-$, 2% Retro$^+$*Drd1*$^-$*Drd2*$^+$, 0.5% Retro$^-$*Drd1*$^-$*Drd2*$^+$, 0.2% Retro$^-$*Drd1*$^+$*Drd2*$^+$).

(G) Selective chemogenetic inhibition of frontal-projecting claustral neurons during encoding inhibits CPP (GFP control n = 6; hM4Di saline n = 6; hM4Di CNO n = 7, paired t test; see also Data S1).

(H) Optogenetic stimulation of claustral neurons projecting to the ACC and OFC drives the development of real-time CPP (n = 6, linear regression model including the mouse and day effects). *p < 0.05, **p < 0.01, ***p < 0.001. See also Figure S5 and Data S1.

acquisition of cocaine CPP (p = 0.24, paired t test). Thus, frontal-projecting claustral neurons are enriched for *Drd1* expression and mediate the allocation of cocaine context association. We were further interested in addressing the capacity of frontal-projecting claustral neurons to support the allocation of incentive salience, using the real-time CPP paradigm (Figure 5H). Similar to our observations with D1-Cre mice, optogenetic stimulation of claustral neurons projecting to frontal cortex drove the development of rtCPP (Figure 5H) ($F_{3,15}$ = 6.1, p = 0.006, two-way ANOVA using the between-subjects factor of the mouse and within-subjects factor of the experiment day; for location of viral transduction and fiber placement see Figure S5C). A control group of mice expressing GFP in place of ChR2 did not develop preference for the laser-paired side (Figure S5D) ($F_{3,9}$ = 0.73, p = 0.56, two-way ANOVA using the between-subjects factor of the mouse and within-subjects factor of the experiment day).

In sum, activity of frontal-projecting claustral neurons subject to dopamine modulation is crucial for the acquisition of cocaine CPP. The activity of this neuronal population is also sufficient for inducing real-time place preference. Together, these results indicate the existence of a dopamine D1R-dependent claustro-frontal projection pathway supporting the acquisition of incentive salience.

DISCUSSION

The claustrum has been demonstrated to function in salience detection and attention and hypothesized to be involved in reward and reinforcement. In addition, the claustrum is recognized for its extensive neuromodulatory input. We find that inhibition of the activity of CL_{Egr2+} neurons attenuates behavioral sensitization to cocaine, providing the first functional association of the claustrum with cocaine-elicited behaviors. We observe inputs to the claustrum from midbrain dopamine regions, consistent with a number of previous reports [13, 21–27]. Addressing the expression of dopamine receptors in the claustrum, we observe broad expression of *Drd1*, as well as sparse expression of *Drd2*. Thus, in contrast to the striatum where a balance exists

Please cite this article in press as: Terem et al., Claustral Neurons Projecting to Frontal Cortex Mediate Contextual Association of Reward, Current Biology (2020), https://doi.org/10.1016/j.cub.2020.06.064

between neurons expressing the Gs-coupled D1 dopamine receptor and neurons expressing the Gi-coupled D2 dopamine receptor [46], the claustrum is biased toward excitatory D1R activity. The claustral dopamine receptor composition we observe is supported by qualitative published observations [25, 29–34]. Exposing mice to cocaine, we observed robustly induced, and broadly correlated expression of the IEGs *Egr2* and *Fos* within claustral neurons. Consistent with these observations, induction of *Fos* expression in claustral neurons has been reported after acute exposure to amphetamine in a novel environment [51], as well as after exposure to a cocaine paired environment [52]. We find that cocaine-induced IEG induction occurs preferentially within claustral dopamine-expressing neurons, providing support for the notion that recruitment of claustral neurons by cocaine depends on the expression of dopamine receptors within them. Furthermore, we find that IEG expression is preferentially correlated to *Drd1* expression. These results implicate the claustrum in the encoding of cocaine experience and allude to a role of the claustrum in incentive salience. Incentive salience is defined as the requirement for attentional resources to be allocated toward a salient context that is associated with a reward [37]. Repeated exposure to drugs of abuse is anticipated to sensitize the recruitment of brain structures involved in the allocation of incentive salience [37, 53]. Consistent with this notion, we observe sensitization of the net induction of IEG expression in the claustrum after repeated exposure to cocaine, further associating the claustrum with attribution of incentive salience.

To address a role for the claustrum in the acquisition and expression of drug reward, we utilized the cocaine CPP assay. We focused on the role of *Drd1*$^+$ neurons, as we found these neurons to be those most robustly recruited by cocaine experience. Dopamine acts on D1Rs through activation of the stimulatory Gs-coupled signaling pathway. Therefore, we studied the impact of inhibiting neuronal excitation in these neurons (through constitutive expression of the Kir2.1 inward-rectifying K^+ channel) or activation of Gi-coupled signaling by stimulation of the inhibitory DREADD hM4Di. We observe that constitutive inhibition of claustral *Drd1*-expressing neurons attenuates cocaine CPP. However, this experiment does not define whether the activity of the claustrum is important for the acquisition or the expression of cocaine preference. To address this, we applied chemogenetics for inhibition of the claustrum during either acquisition or expression of cocaine CPP. We find that the activity of claustral *Drd1*$^+$ neurons is selectively required for the acquisition of cocaine CPP, while being dispensable for the expression of CPP. As a nucleus supporting incentive salience, stimulation of claustral neurons would be anticipated to drive the development of place preference for the context in which the stimulation was engaged. Indeed, we observe clear development of real-time place preference for laser stimulation upon direct optogenetic stimulation of claustral neurons. It is worth mentioning the report of "spatial cells" in the anterior claustrum of the rat [54], as well as the report that claustral neurons projecting to the medial entorhinal cortex are recruited during the encoding of contextual memories [20]. Thus, activity of claustral neurons is recruited during the encoding of context. In the course of attribution of incentive salience, reward-associated contexts likely gain enhanced representation in the claustrum, in a process hijacked by psychostimulants to support sensitization and drug preference.

The claustrum functions as a hub, associating subcortical neuromodulatory inputs and frontal cortical regions. The major projection of the claustrum extends to the ACC and OFC, frontal structures that are strongly associated with salience, attentional allocation, and drug reward [55–62]. Recent evidence implicates claustro-cortico-claustral networks in attention [3,4, 13, 38, 40] and salience [12, 15, 16, 63]. Our results are suggestive of a role for dopaminergic innervation of the claustrum in incentive salience. We further found that dopamine-receptor-expressing claustral neurons project to frontal cortex. In order to pursue the role of the claustrum as a hub supporting the allocation of incentive salience, we addressed the role of frontal-projecting claustral neurons in the development of cocaine CPP. Similar to the observation with D1-Cre mice, we found that the activity of frontal-projecting claustral neurons is required for the acquisition of cocaine CPP. Furthermore, optogenetic activation of frontal-projecting claustral neurons is sufficient to induce context preference. These experiments provide a broader perspective on the role of the claustrum in attribution of incentive salience, overlaying the dopaminergic input to the claustrum onto the frontal projection of the claustrum. Intriguingly, inhibition of claustral neurons projecting to the mPFC has recently been reported to attenuate impulsive behavior induced by exposure of rats to the psychostimulant methamphetamine [64]. These results are consistent with our observations, as they provide additional support for a role of frontal-projecting claustral neurons in mediating the action of psychostimulants.

Thus, cocaine recruits claustral neurons expressing dopamine receptors, and this recruitment is sensitized by repeated cocaine exposure. Claustral neurons expressing dopamine receptors project to frontal cortex and support the acquisition of cocaine and real-time place preference. There is a large body of literature relating to the nucleus accumbens as the central integrator of reward, supporting its role in incentive salience in reinforcement and drug addiction. This raises the question of how our results regarding the role of the claustrum in place preference, and our proposal that the claustrum functions in incentive salience, could relate to the established role of the nucleus accumbens. Although this is largely a topic for future investigation, our perspective is that the functional anatomy of the NAc, with its convergence of dopaminergic, cortical, hippocampal, and amygdalar inputs, and its simple subcortical output, supports its function in reinforcement learning. In contrast, the claustrum exhibits rich reciprocal connectivity with cortex, primarily frontal and association regions, an architecture more amenable to supporting "online" modulation of salience and attention. The claustrum might act to direct attention to reward-related salient cues, promoting the development of a strong association between the reward and its context. The frontal projection of the claustrum has been reported to drive robust feedforward inhibition, dramatically shaping the activity pattern of frontal neurons [40]. Potentially, cocaine-driven allocation of cortical resources increases incentive salience to drug-associated cues by suppressing the activity of frontal cortical resources directed to other, competing objectives. This function might be mediated by dopamine receptors expressed on frontal-projecting claustral neurons, supporting the development of preference for drug-associated contextual cues. Additional circuits, involving direct action of dopamine on frontal cortex, might also function in

incentive salience and might further interact with a dopamine-driven claustro-frontal circuit.

STAR★METHODS

Detailed methods are provided in the online version of this paper and include the following:

- KEY RESOURCES TABLE
- RESOURCE AVAILABILITY
  - Lead Contact
  - Materials Availability
  - Data and Code Availability
- EXPERIMENTAL MODEL AND SUBJECT DETAILS
  - Sex and ages
- METHOD DETAILS
  - Immunohistochemistry
  - Image acquisition
  - Stereotactic surgery and virus injections
  - Midbrain dopamine inputs to the claustrum
  - Behavioral sensitization to cocaine
  - Single molecule fluorescence *in situ* hybridization
  - Conditioned place preference
  - Optogenetics
- QUANTIFICATION AND STATISTICAL ANALYSIS
  - Statistics and Data Analysis
  - smFISH Statistics
  - Behavior Statistics

SUPPLEMENTAL INFORMATION

Supplemental Information can be found online at https://doi.org/10.1016/j.cub.2020.06.064.

ACKNOWLEDGMENTS

The authors appreciate the helpful critical comments of Drs. Inbal Goshen, Segev Barak, Mickey London, Adi Mizrahi, and Eran Lottem, as well as 4 anonymous reviewers, on data, writing, and presentation. We are indebted to Dr. Naomi Book-Melamed, head of the microscopy unit at the Life Science Institute, for technical support in establishing the imaging system required for efficient acquisition of multiplexed smFISH signals. Work in the A.C.'s laboratory is funded by the European Research Council (ERC 770951), The Israel Science Foundation (1062/18, 393/12, 1796/12, and 2341/15), The Israel Anti-Drug Administration, EU Marie Curie (PCIG13-GA-2013-618201), the National Institute for Psychobiology in Israel, Hebrew University of Jerusalem Israel founded by the Charles E. Smith family (109-15-16), an Adelis Award for Advances in Neuroscience, the Brain and Behavior Foundation (NARSAD 18795), German–Israel Foundation (2299-2291.1/2011), and Binational Israel–United States Foundation (2011266), a seed grant from the Eric Roland Fund for interdisciplinary research administered by the ELSC, contributions from anonymous philanthropists in Los Angeles and Mexico City, as well as research support from the Safra Center for Brain Sciences (ELSC) and the Canadian Institute for Advanced Research (CIFAR).

AUTHOR CONTRIBUTIONS

Study Concept and Design, A.T. and A.C.; smFISH, B.J.G. and A.T.; Data Analysis, N.R., R.A.-F., and A.T.; Behavioral Experiments, A.T., D.M., and A.C.; Virus Injection and Cannula Implantation, A.T., N.B., and M.d.M.R.-G.; Virus Preparation, M.d.M.R.-G.; Manuscript Draft, A.T. and A.C.; Funding Acquisition, A.C.; Study Supervision, A.C.

DECLARATION OF INTERESTS

The authors declare no competing interests.

Received: March 27, 2020
Revised: June 1, 2020
Accepted: June 19, 2020
Published: July 23, 2020

REFERENCES

1. Edelstein, L.R., and Denaro, F.J. (2004). The claustrum: a historical review of its anatomy, physiology, cytochemistry and functional significance. Cell. Mol. Biol. *50*, 675–702.
2. Crick, F.C., and Koch, C. (2005). What is the function of the claustrum? Philos. Trans. R Soc. L. B Biol. Sci. *360*, 1271–1279.
3. Mathur, B.N. (2014). The claustrum in review. Front. Syst. Neurosci. *8*, 48.
4. Goll, Y., Atlan, G., and Citri, A. (2015). Attention: the claustrum. Trends Neurosci. *38*, 486–495.
5. Brown, S.P., Mathur, B.N., Olsen, S.R., Luppi, P.H., Bickford, M.E., and Citri, A. (2017). New breakthroughs in understanding the role of functional interactions between the neocortex and the claustrum. J. Neurosci. *37*, 10877–10881.
6. Kim, J., Matney, C.J., Roth, R.H., and Brown, S.P. (2016). Synaptic Organization of the Neuronal Circuits of the Claustrum. J. Neurosci. *36*, 773–784.
7. Reser, D.H., Richardson, K.E., Montibeller, M.O., Zhao, S., Chan, J.M.H., Soares, J.G.M., Chaplin, T., Gattass, R., and Rosa, M.G.P. (2014). Claustrum projections to prefrontal cortex in the capuchin monkey (Cebus apella). Front. Syst. Neurosci. *8*, 123.
8. Chia, Z., Augustine, G.J., and Silberberg, G. (2020). Synaptic Connectivity between the Cortex and Claustrum Is Organized into Functional Modules. Curr. Biol. https://doi.org/10.1016/j.cub.2020.05.031.
9. Smythies, J., Edelstein, L., and Ramachandran, V. (2012). Hypotheses relating to the function of the claustrum. Front. Integr. Neurosci. *6*, 53.
10. Smith, J.B., and Alloway, K.D. (2014). Interhemispheric claustral circuits coordinate sensory and motor cortical areas that regulate exploratory behaviors. Front. Syst. Neurosci. *8*, 93.
11. Citri, A., and Berretta, S. (2016). Claustral Delusions. Claustrum *1*, https://doi.org/10.3402/cla.v1.31426.
12. Patru, M.C., and Reser, D.H. (2015). A new perspective on delusional states: Evidence for claustrum involvement. Front. Psychiatry *6*, 158.
13. Atlan, G., Terem, A., Peretz-Rivlin, N., Sehrawat, K., Gonzales, B.J., Pozner, G., Tasaka, G.I., Goll, Y., Refaeli, R., Zviran, O., et al. (2018). The Claustrum Supports Resilience to Distraction. Curr. Biol. *28*, 2752–2762.
14. White, M.G., Mu, C., Zeng, H., and Mathur, B.N. (2018). The claustrum is required for reward acquisition under high cognitive demand. bioRxiv. https://doi.org/10.1101/390443.
15. Smith, J.B., Watson, G.D.R., Liang, Z., Liu, Y., Zhang, N., and Alloway, K.D. (2019). A role for the claustrum in salience processing? Front. Neuroanat. *13*, 64.
16. Remedios, R., Logothetis, N.K., and Kayser, C. (2010). Unimodal responses prevail within the multisensory claustrum. J. Neurosci. *30*, 12902–12907.
17. Remedios, R., Logothetis, N.K., and Kayser, C. (2014). A role of the claustrum in auditory scene analysis by reflecting sensory change. Front. Syst. Neurosci. *8*, 44.
18. Bray, N. (2018). Concentrating on the claustrum. Nat. Rev. Neurosci. *19*, 580–581.
19. Jackson, J. (2018). Attention: Noisy Networks Are Tuned Out by the Claustrum. Curr. Biol. *28*, R937–R939.
20. Kitanishi, T., and Matsuo, N. (2017). Organization of the claustrum-to-entorhinal cortical connection in mice. J. Neurosci. *37*, 269–280.

21. Baizer, J.S. (2014). The Neurochemical Organization of the Claustrum. In The Claustrum, Chapter 3, J.R. Smythies, L.R. Edelstein, and V.S. Ramachandran, eds. (Academic Press), pp. 85–118.

22. Druga, R. (2014). The Structure and Connections of the Claustrum. In The Claustrum, Chapter 2, J.R. Smythies, L.R. Edelstein, and V.S. Ramachandran, eds. (Academic Press), pp. 29–84.

23. Pirone, A., Miragliotta, V., Ciregia, F., Giannessi, E., and Cozzi, B. (2018). The catecholaminergic innervation of the claustrum of the pig. J. Anat. *232*, 158–166.

24. Sutoo, D., Akiyama, K., Yabe, K., and Kohno, K. (1994). Quantitative analysis of immunohistochemical distributions of cholinergic and catecholaminergic systems in the human brain. Neuroscience *58*, 227–234.

25. Borroto-Escuela, D.O., and Fuxe, K. (2019). On the G Protein-Coupled Receptor Neuromodulation of the Claustrum. Neurochem. Res. *45*, 5–15.

26. Zingg, B., Dong, H.W., Tao, H.W., and Zhang, L.I. (2018). Input-output organization of the mouse claustrum. J. Comp. Neurol. *526*, 2428–2443.

27. Zhang, X., Hannesson, D.K., Saucier, D.M., Wallace, A.E., Howland, J., and Corcoran, M.E. (2001). Susceptibility to kindling and neuronal connections of the anterior claustrum. J. Neurosci. *21*, 3674–3687.

28. Khlghatyan, J., Quintana, C., Parent, M., and Beaulieu, J.M. (2019). High Sensitivity Mapping of Cortical Dopamine D2 Receptor Expressing Neurons. Cereb. Cortex *29*, 3813–3827.

29. Cortimiglia, R., Infantellina, F., Salerno, M.T., and Zagami, M.T. (1982). Unit study in cat claustrum of the effects of iontophoretic neurotransmitters and correlations with the effects of activation of some afferent pathways. Arch. Int. Physiol. Biochim. *90*, 219–230.

30. Fuxe, K., Agnati, L.F., Merlo Pich, E., Meller, E., and Goldstein, M. (1987). Evidence for a fast receptor turnover of D1 dopamine receptors in various forebrain regions of the rat. Neurosci. Lett. *81*, 183–187.

31. Schiffmann, S.N., Libert, F., Vassart, G., Dumont, J.E., and Vanderhaeghen, J.J. (1990). A cloned G protein-coupled protein with a distribution restricted to striatal medium-sized neurons. Possible relationship with D1 dopamine receptor. Brain Res. *519*, 333–337.

32. Weiner, D.M., and Brann, M.R. (1989). The distribution of a dopamine D2 receptor mRNA in rat brain. FEBS Lett. *253*, 207–213.

33. Mijnster, M.J., Isovich, E., Flügge, G., and Fuchs, E. (1999). Localization of dopamine receptors in the tree shrew brain using [3H]-SCH23390 and [125I]-epidepride. Brain Res. *841*, 101–113.

34. Suzuki, M., Hurd, Y.L., Sokoloff, P., Schwartz, J.C., and Sedvall, G. (1998). D3 dopamine receptor mRNA is widely expressed in the human brain. Brain Res. *779*, 58–74.

35. Sitte, H.H., Pifl, C., Rajput, A.H., Hörtnagl, H., Tong, J., Lloyd, G.K., Kish, S.J., and Hornykiewicz, O. (2017). Dopamine and noradrenaline, but not serotonin, in the human claustrum are greatly reduced in patients with Parkinson's disease: possible functional implications. Eur. J. Neurosci. *45*, 192–197.

36. Robinson, T.E., and Berridge, K.C. (1993). The neural basis of drug craving: an incentive-sensitization theory of addiction. Brain Res. Brain Res. Rev. *18*, 247–291.

37. Robinson, T.E., and Berridge, K.C. (2008). Review. The incentive sensitization theory of addiction: some current issues. Philos. Trans. R. Soc. Lond. B Biol. Sci. *363*, 3137–3146.

38. White, M.G., Panicker, M., Mu, C., Carter, A.M., Roberts, B.M., Dharmasri, P.A., and Mathur, B.N. (2018). Anterior Cingulate Cortex Input to the Claustrum Is Required for Top-Down Action Control. Cell Rep. *22*, 84–95.

39. White, M.G., and Mathur, B.N. (2018). Frontal cortical control of posterior sensory and association cortices through the claustrum. Brain Struct. Funct. *223*, 2999–3006.

40. Jackson, J., Karnani, M.M., Zemelman, B.V., Burdakov, D., and Lee, A.K. (2018). Inhibitory Control of Prefrontal Cortex by the Claustrum. Neuron *99*, 1029–1039.

41. Narikiyo, K., Mizuguchi, R., Ajima, A., Shiozaki, M., Hamanaka, H., Johansen, J.P., Mori, K., and Yoshihara, Y. (2020). The claustrum coordinates cortical slow-wave activity. Nat. Neurosci. *23*, 741–753.

42. Wang, Q., Ng, L., Harris, J.A., Feng, D., Li, Y., Royall, J.J., Oh, S.W., Bernard, A., Sunkin, S.M., Koch, C., et al. (2017). Organization of the Connections Between Claustrum and Cortex in the Mouse. J. Comp. Neurol. *525*, 1317–1346.

43. Atlan, G., Terem, A., Peretz-Rivlin, N., Groysman, M., and Citri, A. (2017). Mapping synaptic cortico-claustral connectivity in the mouse. J. Comp. Neurol. *525*, 1381–1402.

44. Poulin, J.F., Caronia, G., Hofer, C., Cui, Q., Helm, B., Ramakrishnan, C., Chan, C.S., Dombeck, D.A., Deisseroth, K., and Awatramani, R. (2018). Mapping projections of molecularly defined dopamine neuron subtypes using intersectional genetic approaches. Nat. Neurosci. *21*, 1260–1271.

45. Mukherjee, D., Ignatowska-Jankowska, B.M., Itskovits, E., Gonzales, B.J., Turm, H., Izakson, L., Haritan, D., Bleistein, N., Cohen, C., Amit, I., et al. (2018). Salient experiences are represented by unique transcriptional signatures in the mouse brain. eLife *7*, https://doi.org/10.7554/eLife.31220.

46. Gonzales, B.J., Mukherjee, D., Ashwal-Fluss, R., Loewenstein, Y., and Citri, A. (2019). Subregion-specific rules govern the distribution of neuronal immediate-early gene induction. Proc. Natl. Acad. Sci. USA. https://doi.org/10.1073/pnas.1913658116.

47. Kravitz, A.V., Tye, L.D., and Kreitzer, A.C. (2012). Distinct roles for direct and indirect pathway striatal neurons in reinforcement. Nat. Neurosci. *15*, 816–818.

48. Wang, Q., Ng, L., Harris, J.A., Feng, D., Li, Y., Royall, J.J., Oh, S.W., Bernard, A., Sunkin, S.M., Koch, C., et al. (2017). Organization of the connections between claustrum and cortex in the mouse. J. Comp. Neurol. *525*, 1317–1346.

49. Mathur, B.N., Caprioli, R.M., and Deutch, A.Y. (2009). Proteomic analysis illuminates a novel structural definition of the claustrum and insula. Cereb. Cortex *19*, 2372–2379.

50. Smith, J.B., Liang, Z., Watson, G.D.R., Alloway, K.D., and Zhang, N. (2017). Interhemispheric resting-state functional connectivity of the claustrum in the awake and anesthetized states. Brain Struct. Funct. *222*, 2041–2058.

51. Badiani, A., Oates, M.M., Day, H.E.W., Watson, S.J., Akil, H., and Robinson, T.E. (1998). Amphetamine-induced behavior, dopamine release, and c-fos mRNA expression: modulation by environmental novelty. J. Neurosci. *18*, 10579–10593.

52. Brown, E.E., Robertson, G.S., and Fibiger, H.C. (1992). Evidence for conditional neuronal activation following exposure to a cocaine-paired environment: role of forebrain limbic structures. J. Neurosci. *12*, 4112–4121.

53. Tindell, A.J., Berridge, K.C., Zhang, J., Peciña, S., and Aldridge, J.W. (2005). Ventral pallidal neurons code incentive motivation: amplification by mesolimbic sensitization and amphetamine. Eur. J. Neurosci. *22*, 2617–2634.

54. Jankowski, M.M., and O'Mara, S.M. (2015). Dynamics of place, boundary and object encoding in rat anterior claustrum. Front. Behav. Neurosci. *9*, 1–19.

55. Goldstein, R.Z., and V.N.. (2011). Prefronal cortex, addiction. Nat. Rev. Neurosci. *12*, 652–669.

56. Seeley, W.W., Menon, V., Schatzberg, A.F., Keller, J., Glover, G.H., Kenna, H., Reiss, A.L., and Greicius, M.D. (2007). Dissociable intrinsic connectivity networks for salience processing and executive control. J. Neurosci. *27*, 2349–2356.

57. Goldstein, R.Z., Tomasi, D., Rajaram, S., Cottone, L.A., Zhang, L., Maloney, T., Telang, F., Alia-Klein, N., and Volkow, N.D. (2007). Role of the anterior cingulate and medial orbitofrontal cortex in processing drug cues in cocaine addiction. Neuroscience *144*, 1153–1159.

58. Baeg, E., Jedema, H.P., and Bradberry, C.W. (2019). Orbitofrontal cortex is selectively activated in a primate model of attentional bias to cocaine cues. Neuropsychopharmacology *45*, 675–682.

59. Grant, S., London, E.D., Newlin, D.B., Villemagne, V.L., Liu, X., Contoreggi, C., Phillips, R.L., Kimes, A.S., and Margolin, A. (1996). Activation of memory circuits during cue-elicited cocaine craving. Proc. Natl. Acad. Sci. USA *93*, 12040–12045.

60. Maas, L.C., Lukas, S.E., Kaufman, M.J., Weiss, R.D., Daniels, S.L., Rogers, V.W., Kukes, T.J., and Renshaw, P.F. (1998). Functional magnetic resonance imaging of human brain activation during cue-induced cocaine craving. Am. J. Psychiatry *155*, 124–126.

61. Baeg, E.H., Jackson, M.E., Jedema, H.P., and Bradberry, C.W. (2009). Orbitofrontal and anterior cingulate cortex neurons selectively process cocaine-associated environmental cues in the rhesus monkey. J. Neurosci. *29*, 11619–11627.

62. Schoenbaum, G., and Shaham, Y. (2008). The role of orbitofrontal cortex in drug addiction: a review of preclinical studies. Biol. Psychiatry *63*, 256–262.

63. Chia, Z., Silberberg, G., and Augustine, G.J. (2017). Functional properties, topological organization and sexual dimorphism of claustrum neurons projecting to anterior cingulate cortex. Claustrum *2*, 1357412.

64. Liu, J., Wu, R., Johnson, B., Vu, J., Bass, C., and Li, J.X. (2019). The Claustrum-Prefrontal Cortex Pathway Regulates Impulsive-Like Behavior. J. Neurosci. *39*, 10071–10080.

65. Pollak Dorocic, I., Fürth, D., Xuan, Y., Johansson, Y., Pozzi, L., Silberberg, G., Carlén, M., and Meletis, K. (2014). A whole-brain atlas of inputs to serotonergic neurons of the dorsal and median raphe nuclei. Neuron *83*, 663–678.

66. Paxinos, G., and Franklin, K.B.J. (2013). The Mouse Brain in Stereotaxic Coordinates. (Wiley).

67. Turm, H., Mukherjee, D., Haritan, D., Tahor, M., and Citri, A. (2014). Comprehensive Analysis of Transcription Dynamics from Brain Samples Following Behavioral Experience. J. Vis. Exp. https://doi.org/10.3791/51642.

68. Kamentsky, L., Jones, T.R., Fraser, A., Bray, M.A., Logan, D.J., Madden, K.L., Ljosa, V., Rueden, C., Eliceiri, K.W., and Carpenter, A.E. (2011). Improved structure, function and compatibility for CellProfiler: modular high-throughput image analysis software. Bioinformatics *27*, 1179–1180.

69. Kravitz, A.V., and Kreitzer, A.C. (2012). Striatal mechanisms underlying movement, reinforcement, and punishment. Physiology *27*, 167–177.

Please cite this article in press as: Terem et al., Claustral Neurons Projecting to Frontal Cortex Mediate Contextual Association of Reward, Current Biology (2020), https://doi.org/10.1016/j.cub.2020.06.064

STAR★METHODS

KEY RESOURCES TABLE

REAGENT or RESOURCE	SOURCE	IDENTIFIER
Antibodies		
Rabbit anti-TH	Merck Millipore	Cat#AB152; RRID: AB_390204
donkey anti-rabbit IgG H&L Alexa Fluor 488	Abcam	Cat#ab150065
Bacterial and Virus Strains		
AAVdj-DIO-eGFP	Vector core facility of the Edmond and Lily Safra Center for Brain Sciences	N/A
AAVdj-EF1a-DIO-Kir2.1-t2A-zsGreen	Stanford viral core facility	N/A
AAV2-hSyn-DIO-hM4D(Gi)-mCherry	UNC	AV-4-500a
AAV2-hSyn-DIO-hM4D(Gi)-mCherry	Vector core facility of the Edmond and Lily Safra Center for Brain Sciences	N/A
retroAAV-CKII-iCre	Vector core facility of the Edmond and Lily Safra Center for Brain Sciences	N/A
AAV9-CAGGS-FLEX-ChR2-TdTomato	UPENN	AV-9-18917P
Deposited Data		
Original data have been deposited to Mendeley Data	This paper	https://doi.org/10.17632/4d6wm9ggkr.1; https://doi.org/10.17632/cf8kzg53m2.1; https://doi.org/10.17632/xbh3bnt3gk.1; https://doi.org/10.17632/3w6j9hwcmy.1; https://doi.org/10.17632/kfjhvvpfj6.1; https://doi.org/10.17632/5f4999f44m.1; https://doi.org/10.17632/t549jrw4p3.1
Experimental Models: Organisms/Strains		
PVcre:Ai9	The Jackson Laboratory	Stock No. 017320; Stock No:007909; RRID: IMSR_JAX:017320; RRID: IMSR_JAX:007909
DAT-IRES-cre	The Jackson Laboratory	Stock No:006660; RRID: IMSR_JAX:006660
Krox20-Cre (Egr2-CRE)	The Jackson Laboratory	Stock No:025744; RRID: IMSR_JAX:025744
D1-cre	The Jackson Laboratory	Stock No:37156-JAX; RRID: MMRRC_037156-JAX
Oligonucleotides		
Probe- Mm-EGFP	RNAscope®	Cat#400281
Probe- Mm-Slc17a7-C2	RNAscope®	Cat#416631-C2
Probe- Mm-Egr2	RNAscope®	Cat#407871
Probe- Mm-Drd1a-C2	RNAscope®	Cat#406491-C2
Probe- Mm-Drd1a-C3	RNAscope®	Cat#406491-C3
Probe- Mm-Fos-C3	RNAscope®	Cat#316921-C3
Software and Algorithms		
The R Project for Statistical Computing		https://www.r-project.org software
Photoshop, Illustrator, and InDesign	Adobe, San Jose, CA	
CellProfiler	Broad Institute	

RESOURCE AVAILABILITY

Lead Contact

Further information and requests for resources and reagents should be directed to and will be fulfilled by the Lead Contact, Ami Citri (ami.citri@mail.huji.ac.il).

Please cite this article in press as: Terem et al., Claustral Neurons Projecting to Frontal Cortex Mediate Contextual Association of Reward, Current Biology (2020), https://doi.org/10.1016/j.cub.2020.06.064

Materials Availability

This study did not generate new unique reagents.

Data and Code Availability

Original data have been deposited to Mendeley Data under the following: https://doi.org/10.17632/4d6wm9ggkr.1; https://doi.org/10.17632/cf8kzg53m2.1; https://doi.org/10.17632/xbh3bnt3gk.1; https://doi.org/10.17632/3w6j9hwcmy.1; https://doi.org/10.17632/kfjhvvpfj6.1; https://doi.org/10.17632/5f4999f44m.1; https://doi.org/10.17632/t549jrw4p3.1. Data is also available from the lead contact upon request.

EXPERIMENTAL MODEL AND SUBJECT DETAILS

Mice described in this study were C57BL/6 inbred mice purchased from Harlan Laboratories or transgenic mouse lines, as indicated. Transgenic lines included Ai9xPV-Cre (PV-Cre mice crossed to the reporter mouse line Ai9, expressing Cre-dependent tdTomato), DAT-Cre, Egr2-Cre and D1-Cre. All mice were maintained on a 12-hour light-dark cycle in a specific pathogen-free (SPF) animal facility with free access to food and water. All experimental procedures, handling, surgeries and care of laboratory animals used in this study were approved by the Hebrew University Institutional Animal Care and Use Committee (IACUC).

Sex and ages

Connectivity experiment

Male, 6 weeks old at the time of virus injections.

Behavioral sensitization to cocaine experiment

Male, aged 6-8 weeks old at the time of virus injections.

Single molecule fluorescence in situ hybridization experiments

Male, aged 5-7 weeks old.

Conditioned place preference experiments

Male, aged 6-8 weeks old at the time of virus injections.

Optogenetics experiments

Male, aged 8-12 weeks old at the time of virus injections and cannula implantation.

Each experiment was conducted on homogeneous cohorts and individual mice were randomly assigned to experimental groups.

METHOD DETAILS

Immunohistochemistry

Mice were anesthetized with 5% isoflurane, followed by rapid decapitation. Brains were removed and fixed in 4% PFA overnight at 4°C. On the following day, brains were thoroughly rinsed in a 0.9% NaCl Phosphate buffered saline (PBS) solution and sectioned on a Vibratome (7000 smz-2) at 60μM thickness in the coronal plane. Two series of sections were collected from each brain, resulting in two copies of brain slices at 120μm apart, corresponding to the division of the mouse brain atlas (as in [65]). In order to stain for TH, floating section immunohistochemistry was performed. Sectioned brain slices were washed twice in PBS, followed by blocking in 3% normal horse serum and 0.3% Triton X-100 in PBS for 1 hour. Sections were then incubated overnight at 4°C in a rabbit anti-TH primary antibody (TH antibody Merck Millipore, cat. #AB152, final dilution to 1:500 in 3% normal horse serum). 16 hr later the sections were washed three times in PBS. Washes were followed by 2 hours of incubation at room temperature with donkey anti-rabbit IgG H&L Alexa Fluor 488 (Abcam; catalog No. ab150065; final dilution to 1:500) in 3% normal horse serum. Finally, the sections were washed three times in PBS and then counterstained with DAPI (Roche; catalog No. 10-236-276; final dilution 1:1000 in PBS) to detect cell nuclei and then quickly washed twice, mounted onto slides and covered.

Image acquisition

Slides were scanned on a high-speed fully-motorized multi-channel light microscope (Olympus IX-81) in the microscopy unit of the Alexander Silberman Institute of Life Sciences. 10X magnification (NA = 0.3), 20X magnification (NA = 0.5) or 40X magnification (NA = 0.6). Green and red channels exposure times were selected for optimal clarity and were kept constant within each brain series. DAPI was acquired using excitation filters of 350 ± 50nm, emission 455 ± 50nm; GFP excitation 490 ± 20nm, emission 525 ± 36; mCherry/tdTomato excitation 555 ± 25nm, emission 605 ± 52nm. Figures were prepared using Photoshop, Illustrator, and InDesign (Adobe, San Jose, CA). Figures showing stained brain tissue were adjusted using a uniform brightness/contrast mask created in linear-mode in Photoshop, and applied consistently to all slices within a single brain. Images were then scaled or cropped to improve data presentation and increase signal visibility. Digitization was performed from raw, non-adjusted images.

Stereotactic surgery and virus injections

Mice were anesthetized by IP injection of ketamine (75 mg/kg) and medetomidine (1 mg/kg). Following validation of the depth of anesthesia, mice were secured in a stereotaxic apparatus (David KOPF instruments, Tujunga CA). Following incision of the scalp,

a small hole was made in the skull using a fine drill burr (model 78001, RWD Life Science, San Diego CA). A microsyringe (33GA Hamilton syringe, Reno, NV) loaded with the virus was lowered into the target structure. The viral tracer was injected at 50-100nl/min via an UltraMicroPump (World Precision Instruments, Saratosa, FL), following which the microsyringe was left in the tissue for 5 minutes after the termination of the injection before being slowly retracted. Finally, the incision was closed with bioadhesive and the animals were injected with saline (for hydration), antisedan (to negate the anesthesia) and rimadyl (analgesic) and recovered under gentle heating. Coordinates for stereotactic injection were based on the Paxinos and Franklin mouse brain atlas [66]. The coordinates used for claustral injections were LM: ± 2.8mm, RC: 1mm, DV: −3.7mm relative to Bregma. Unless noted otherwise, viruses were prepared at the vector core facility of the Edmond and Lily Safra Center for Brain Sciences, as described previously [43].

Midbrain dopamine inputs to the claustrum

Inputs to the claustrum from midbrain dopamine neurons were analyzed by stereotactic targeting of AAV-DIO-GFP to the midbrain of DAT-Cre mice. Coordinates used to target the SN were (relative to Bregma) LM: ± 1.3mm, RC: −3mm, DV: −4.75mm (Figure 1D). These results were further corroborated by publicly available data found on the online repository of the Allen Mouse Brain Connectivity Atlas (experiments: 158314987; 267538735; 165975096; 264696942; 158914182). Images from two experiments (158314987, 158914182) are shown in Figure S1.

Behavioral sensitization to cocaine

The experimental group of CL_{Egr2+} inhibition comprised of (n = 9) Egr2-Cre male mice, aged 6-8 weeks, which were bilaterally injected with 100nl AAVdj-CAG-DIO-GPE2 (Kir2.1) to the claustrum, (LM: ± 2.8mm, RC: 1mm, DV: −3.7). As a control group, (n = 6) Egr2-Cre male mice, 6-8 weeks old, were injected with 100nl AAVdj-CAG-DIO-eGFP to the same coordinates. Animals were randomly assigned to control and experimental group.

Before the start of an experiment, mice were acclimated to the animal facility for 5 days, followed by 3 days of experimenter handling once daily. Animals were then subjected to three days of intraperitoneal (IP) saline injections (250 μl/injection) and transferred to a video-recorded open field arena for 15 minutes (as in [45, 67]). Mice received cocaine (IP, 20 mg/kg freshly dissolved in 0.9% saline to 2 mg/ml, injected at a volume of 10 ml/kg), transferred to the open field arena for 15 minutes to measure locomotor behavior. Locomotor activity was assessed in sound- and light- attenuated open-field chambers. Mice were placed individually in a clear, dimly lit Plexiglas box (30 × 30 × 30 cm) immediately after the IP injection of saline or cocaine. Activity was monitored with an overhead video camera for a total of 15 minutes while the mice were in the open field chamber using Ethovision software (Noldus, Wageningen, Netherlands). Cocaine was purchased from the pharmacy at Hadassah Hospital, Jerusalem. No experimental mice were excluded from analysis.

Single molecule fluorescence *in situ* hybridization

Mice

Animals were sacrificed either directly from the homecage (0hr) or 1hr following their first exposure to cocaine (20 mg/kg, IP; 'Acute'). 'Repeated 1hr' mice were sacrificed an hour after their 5th daily exposure to cocaine, compared to 'Repeated 0hr', which received 4 days of cocaine, and were sacrificed on the 5th day directly from home cage. 'Challenge' mice were sacrificed after 21 days of abstinence from repeated exposure to cocaine, either directly from the homecage (0hr) or 1hr after one final re-exposure to cocaine. n = 3 mice in each group. In all experiments 0hr and 1hr are different groups of mice, from the same cohort. Sections: *Egr2*: Acute (0hr; n = 9, 1hr; n = 9), Repeated (0hr; n = 9, 1hr; n = 9), Challenge (0hr; n = 6, 1hr; n = 8), *Fos*: Acute (0hr; n = 6, 1hr; n = 6), Repeated (0hr; n = 6, 1hr; n = 6), Challenge (0hr; n = 4, 1hr; n = 6), *Drd1*: Acute (0hr; n = 6, 1hr; n = 6), Repeated (0hr; n = 6, 1hr; n = 6), Challenge (0hr; n = 4, 1hr; n = 5), *Drd2*: Acute (0hr; n = 6, 1hr; n = 6), Repeated (0hr; n = 6, 1hr; n = 6), Challenge (0hr; n = 4, 1hr; n = 5). Cells: *Egr2*: Acute (0hr; n = 2428, 1hr; n = 2392), Repeated (0hr; n = 2082, 1hr; n = 2242), Challenge (0hr; n = 1793, 1hr; n = 2326), *Fos*: Acute (0hr; n = 1632, 1hr; n = 1581), Repeated (0hr; n = 1353, 1hr; n = 1507), Challenge (0hr; n = 1150, 1hr; n = 1714); *Drd1*: Acute (0hr; n = 1638, 1hr; n = 1626), Repeated (0hr; n = 1397, 1hr; n = 1456), Challenge (0hr; n = 1231, 1hr; n = 1439), *Drd2*: Acute (0hr; n = 1586, 1hr; n = 1577), Repeated (0hr; n = 1414, 1hr; n = 1521), Challenge (0hr; n = 1205, 1hr; n = 1499). *vGlut1/Drd1*: n = 2 slices: cells: n = 1494. RetroAAV: Mice: n = 2, Slices: n = 4; cells n = 4860.

Staining

The smFISH protocol was implemented according to manufacturer guidelines (ACD RNAscope fresh frozen tissue pretreatment and fluorescent multiplex assay manuals; catalog #320513, #320293; as in Gonzales 2019). Mice were deeply anesthetized with isoflurane, decapitated, their brains rapidly removed and briefly washed in ice-cold PBS. Brains were then placed in molds containing OCT embedding medium (Scigen Scientific Gardena, CA 90248 U.S.A) and snap frozen on dry ice. Embedded brains were sectioned on a Leica CM1950 cryostat into 14μ sections, mounted onto SuperfrostTM Plus slides (#J1800AMNZ) and stored at −80°C. Adjacent sections (at ~0.8 ± 0.3 from Bregma) were processed for probe hybridization. All probes and kits were purchased from Advanced Cell Diagnostics (Mm-Egr2 #407871, Mm-EGFP #400281, Mm-Drd1a-C2 #406491-C2, Mm-Drd1a-C3 #406491-C3 (targeting the Drd1a isoform), Mm-Drd2-C2 #406501-C2, Mm-Slc17a7-C2#416631-C2, Mm-Fos-C3#316921-C3, Fluorescent Multiplex Reagent Kit #320850). Slides were counterstained with DAPI for 30 s and coverslipped with mounting medium (Lab VisionTM PermaFluorTM Aqueous Mounting Medium, #TA-030-FM). Sections were imaged with the Hermes high definition cell-imaging system using a 10x 0.4NA and 40X 0.75NA objectives, to capture 5 Z stack images in each of 4 different channels-475/28 nm (FITC), 549/15 nm (TRITC), 648/20 nm (Cy5) & 390/18 nm (DAPI). Single images for each channel were obtained using Maximum Intensity Z-projection in ImageJ.

Please cite this article in press as: Terem et al., Claustral Neurons Projecting to Frontal Cortex Mediate Contextual Association of Reward, Current Biology (2020), https://doi.org/10.1016/j.cub.2020.06.064

Maximum intensity images were merged, and the claustrum region was manually cropped using ImageJ according to the Franklin and Paxinos Mouse brain atlas, Third edition [66]. Images were analyzed using the CellProfiler speckle counting pipeline [68].

The boundaries of the claustrum were defined for coronal sections located 0.8 ± 0.3mm rostral to Bregma, adhering to the following criteria, with subtle adjustment according to cues obtained from cell density and morphology:

Medio-lateral axis

The claustrum is approximate to the corpus callosum, defining a clear border between the striatum and the claustrum. The lateral extent of the claustrum is defined as one third of the length between the corpus callosum and the lateral border of the cortex.

Dorso-ventral axis

the dorsal boundary of the claustrum is defined as the ventral tip of the broad aspect of the corpus callosum, at a position where a vertical tangent would meet the convex curvature of the corpus callosum. The ventral boundary of the claustrum is horizontal to the dorsal curve of the anterior commissure.

Conditioned place preference

Apparatus

Each place conditioning apparatus consists of an open field enclosed in separate light- and sound-attenuating chambers. General activity and location in the open field was monitored by video recording. The floor of the open field consisted of interchangeable halves made of one of two textures. The combination of floor textures was selected on the basis of calibration studies observing that mice spend an average of about 50% time on each floor type during preference tests. Thus, the apparatus is ''unbiased.'' Specifically, the floors are either of a rough ''crushed ice'' texture, coupled with walls on which appear black dots versus a smooth floor texture coupled with walls on which appear vertical black lines. Prior to and following each session the open field and floors was cleaned using a solution of 5% virusolve.

Experiment	Viruses	Coordinates:	n#	Strain
Constitutive inhibition	AAVdj-DIO-eGFP	±2.82,1,-3.69	GFP = 7	D1- Cre
	AAVdj-CAG-DIO-GPE2 (Kir2.1)		Kir2.1 = 7	
Chemogenetic inhibition during acquisition	AAV2-hSyn-DIO-hM4Di	±2.82,1,-3.69	GFP/CNO = 5	D1- Cre
			hM4Di/Saline = 7	
			hM4Di/CNO = 7	
Chemogenetic inhibition during expression	AAV2-hSyn-DIO-hM4Di	±2.82,1,-3.69	WT = 7	D1- Cre
			hM4Di/CNO = 5	
Chemogenetic inhibition during acquisition	retroAAV-CKII-iCre AAV2-hSyn-DIO-hM4Di	ACC: ± 0.25,1,-1.75	GFP/CNO = 6	WT
		OFC: ± 1,2.55,-2.4	hM4Di/Saline = 6	
		CLA: ± 2.8,1,-3.7	hM4Di/CNO = 7	

Procedures

An unbiased conditioning procedure consists of the following phases:

Handling

30-min sessions. *Pre-conditioning bias test:* a single 20 min test session is conducted during which mice are allowed to freely explore the open field with half of the arena containing the ''crushed ice'' floor and dots walls and half of the arena containing the ''smooth'' floor and straight lines walls. *Conditioning:* 3 days 2 session/day. Mice are randomly assigned to one of two groups, pairing cocaine (10 mg/kg IP) to either the 'crushed ice' or 'smooth' contexts, while saline conditioning (10 ml/kg) occurred on the opposite context. On all sessions, mice have access to the entire apparatus with the same floor and walls type on both sides. *Post-conditioning bias test:* identical to *Pre-conditioning.* Each CPP experiment was performed on a different group of mice, where *Pre-conditioning* and *Post-conditioning bias test* was measured within the same group of mice. For chemogenetic inhibition during conditioning, CNO (10 mg/kg, IP) was injected 30min prior to cocaine. For chemogenetic inhibition during expression, mice went through the regular CPP protocol, including a retrieval test, following which they were subject to another conditioning day and finally, to an additional test 30min after CNO (10 mg/Kg, IP) injection. A single mouse from the h4MDi retroAAV-CRE CNO group was excluded as no infection was observed upon validation.

Optogenetics

Surgery

At 8-12 weeks of age mice were stereotactically injected for real-time CPP (rtCPP) experiments. The first experimental cohort consisted of D1-Cre male mice (n = 8) stereotactically injected with 80nl of AAV9-CAGGS-FLEX-ChR2-TdTomato (purchased from the UPENN virus core) to the claustrum region (LM: 2.82, RC: 1, DV: −3.7). The second experimental cohort consisted of WT

c57/bl6 mice (n = 6) stereotactically injected with 200nl retroAAV-CKII-iCre to the ACC (LM: ± 0.25, RC: 1.1, DV: −1.9) and OFC (LM: ± 1, RC: 2.55, DV: −2.4) and 80nl of AAV9-CAGGS-FLEX-ChR2-TdTomato stereotactically injected to the claustrum region (LM: ± 2.82, RC: 1, DV: −3.7). The control group consisted of 4 WT c57/bl6 mice stereotactically injected with 200nl retroAAV-CKII-iCre to the ACC (LM: ± 0.25, RC: 1.1, DV: −1.9) and OFC (LM: ± 1, RC: 2.55, DV: −2.4) and 80nl of AAV9-CAGGS-FLEX-ChR2-TdTomato stereotactically injected to the claustrum region (LM: ± 2.82, RC: 1, DV: −3.7). Silica multimode fiber optic cannula (200-μm core; 240-μm outer diameter) mounted in a 1.25-mm zirconia ferrule (Doric lenses) were slowly lowered into the brain bilaterally following virus injection (LM: ± 2.82, RC: 1, DV: −3.65), and cemented in place such that the fiber tip was located above the claustrum.

Optogenetics equipment

A blue laser (MBL-FN-437-200mW, CNI laser), was connected to 1x2 Intensity Division Fiberoptic Rotary Joint (FRJ_1x2i_SMA-2FC_0.22, Doric). Two 50cm Mono Fiberoptic Patchcord (MFP_200/230/900-0.37_0.5m_FC-ZF1.25(F), Doric) were connected to the implanted cannulae with a zirconia connection sleeve (1.25mm, Doric).

Real-time CPP

A 3-chamber compartment was used. The north chamber had a smooth floor and walls textured with black and white vertical stripes, while the south chamber had a grid floor and white walls with black dots. The central chamber lacked discerning features and was meant to increase the division between the lateral chambers. Either the north or south chambers were paired with laser stimulation of the claustrum, counterbalanced within each experimental group. The mouse's position was calculated in real time with Ethovision XT 11.5 software. The laser (5mW) was illuminated in a cycle of 1second on / 3second off for the duration that the mouse remained in the laser-paired chamber (as in [69]). All experimental sessions were 20min long. For each real-time CPP experiment repeated-measurements were performed on the same group of mice. No experimental mice were excluded from analysis.

QUANTIFICATION AND STATISTICAL ANALYSIS

Statistics and Data Analysis

R version 3.6.1 was used for all statistical analysis and graphical representations using 'ggplot2'. Description of the statistical analysis models and results for each of the figures is summarized in Data S1.

smFISH Statistics

For the smFISH IEG probes, selection of 'expressing' cells was performed as follows: Addressing control data, removing non-expressing cells (cells expressing 0-1 puncta), the remaining cells were binned equally into three groups based on the per-cell expression levels, and the top 33% cells were defined 'robust expressors'. Thus cells qualified as 'expressors' for a given IEG if they expressed at least the following number of puncta per cell: *Egr2* - 5, *Fos*- 8. For *Drd1, Drd2* & *vGlut1* expression, cells were considered to be positive if they expressed at least 6 puncta per cell (relevant to Figures 2, 3, 5, and S2).

Expression density (Figure 2D) was calculated using Two-Dimensional Kernel Density Estimation with the function 'geom_density_2d' in R. This function estimates two-dimensional kernel density with an axis-aligned bivariate normal kernel, evaluated on a square grid, while displaying the result with contours. The regions of highest density, within which at least 10% of the 'robust expressors' cells are found, were selected. This process was performed independently for each one of the replicas and the selected contours plotted and overlaid (as in [46]).

In order to evaluate the impact of cocaine experience on induction of IEG expression (Figure 3B), we utilized a Student's t test. We further addressed the sensitization of fold-induction of *Egr2* and *Fos* following repeated exposure to cocaine (Figures S3A and S3B) utilizing ANOVA followed by Tukey's test. Evaluation of the effect of long term exposure to cocaine on *Drd1* and *Drd2* expression (Figures S2C and S2D) was performed using ANOVA. Correlations between IEG expression and dopamine receptor expression levels (Figures S3C–S3G) were analyzed by developing a linear model of the data, including the effect of the contribution of individual mice. The resulting coefficient of fit for the gene (relevant probe for each model) and R^2 are reported within the figure. Comparison of the fits between control and cocaine conditions was performed using a mixed-effect model including the random effect of the mouse and fixed effect of treatment (±cocaine) and gene, as well as the interaction treatment:gene. A significant interaction indicates that the slopes differ between conditions (see also Data S1).

Comparison of the proportions of *Egr2*$^+$ cells expressing combinations of dopamine receptors (*Drd1*$^+$ / *Drd2*$^+$ / *Drd1*$^+$&*Drd2*$^+$ / *Drd1*$^-$&*Drd2*$^-$) to their total distribution in the population was performed using a chi-square analysis ($p < 0.0001$; Figure 3F) demonstrating that the proportions were distributed differently between *Egr2*$^+$ cells and the total population. This was followed by a t test to identify the particular fractions which were significantly enriched (or depleted) in the *Egr2*$^+$ cell population. Comparison of the enrichment within the *Egr2*$^+$ cell population in contrast to the total cellular population was also performed for each individual data point (acute/chronic/challenge ± cocaine) implementing a model including the effects of the mouse and condition (experiment and treatment). ANOVA analysis demonstrated enrichment of *Drd1*$^+$ expression within the *Egr2*$^+$ population without significant effect of the interactions with experiment and treatment, indicating that the enrichment in the *Egr2*$^+$ population is independent of these conditions (data not shown; see also Data S1).

Venn diagrams were created in order to represent the fraction of total claustral cells expressing each probe (Figures 5B and 5F) using "eulerr" package in R. The area of the external circle within each panel represents the total number of cells analyzed (based on DAPI staining) while the internal circles represent the fraction of total cells represented by each population.

Please cite this article in press as: Terem et al., Claustral Neurons Projecting to Frontal Cortex Mediate Contextual Association of Reward, Current Biology (2020), https://doi.org/10.1016/j.cub.2020.06.064

Behavior Statistics

In order to evaluate the significance of the impact of Kir2.1 expression on development of behavioral sensitization (Figure 1B), we applied a mixed-effect linear regression model including the mouse as a random effect as well as group and injection day as fixed effects and their interaction. The effect of the manipulation is evaluated by the interaction, representing the difference between the test and control groups in the induction of locomotion following cocaine. Interaction p values of ANOVA and model coefficients are reported in the Data S1.

In order to evaluate the impact of inhibition of claustral neurons on the development of cocaine CPP (Figures 4C, 4D, and 5H) we applied a paired Student's t test, since the objective of the experiment was to address the capacity of each group of mice (experimental or control) to develop CPP (see also Data S1). We further probed the statistics of these experiments, utilizing a preference score (post-test minus pre-test scores) and also performed ANOVA to comparatively address the magnitude of induction of CPP between groups within the same experiment. We used a linear model addressing preference score (pre-test minus post-test) as the dependent variable and testing for the effect of group. This analysis identifies differences in the magnitude of CPP between the Kir2.1 D1-CRE experimental group and the GFP control group ($F_{1,12} = 7.02$, p = 0.021, linear model addressing preference score (pre-test minus post-test) as the dependent variable and testing for the effect of group (Kir2.1 versus GFP), Figure 4C). With regard to the h4MDi D1-CRE and retroAAV experiments – we performed an ANOVA analysis including the effect of the groups as well as the pre-test score of each condition. The differences between the experimental h4MDi-CNO group and the control groups GFP-CNO and h4MDi-saline fell slightly short of providing a significant p value (Figure 4D: $F_{2,15} = 3$, p = 0.08, Figure 5H: $F_{2,16} = 2.71$, p = 0.09). Therefore, in order to further validate our conclusion that CPP developed in the control groups, but failed to develop in the experimental group, we simulated CPP score data and tested for the probability of obtaining these results in a random sampling. For each condition we generated a reference set of random preference score and evaluated the probability of obtaining the observed results by chance. The procedure was performed as following: in order to control for the specific bias of preference in each condition we used the same pre-test scores as in the experiment and sample random post-test values. The range of values used for random sampling were: maximum value as observed in the experiment and minimum value of 1200 minus max value. For each random sample we calculated the differences post-test minus pre-test score. After repeating this process for all samples in each condition we calculated the mean preference score for this condition. We repeated this process for 10,000 iterations to obtain a distribution of random data. p value was defined as the probability of the experimental data to be found within the randomly distributed data (Figure 4D: h4MDi/CNO p = 0.24; h4MDi/Saline p = 0.0007; GFP/CNO p = 0.007, Figure 5G: h4MDi/CNO p = 0.2; h4MDi/Saline p = 0.0008; GFP/CNO p = 0.08).

To address the significance of claustrum inhibition on expression of cocaine CPP (involving repeated-measures, Figure 4E) we applied a separate linear regression model for each mouse group. We included both mouse and day effects. The effects of interest are day effects representing the change in the score between pre-test to each of the other days. Similarly, addressing the impact of inhibition of claustral neurons projecting to frontal cortex on the development of CPP (Figures 4G, 5I, and S5D), we applied a separate linear regression model for each mouse group. We included both mouse and day effects. The effects of interest are day effects representing the change in the score between pre-test to each of the other days. In both test groups (Figures 4G and 5I; see also Data S1) we observed significant day effects whereas no significant day effect was observed in the control group (Figure S5D, see also Data S1).